SAE INTERNATIONAL®

An Experimental and Computational Investigation of Water Condensation inside the Tubes of an Automotive Compact Charge Air Cooler

2016-01-0224
Published 04/05/2016

Robin Y. Cash
Ford Motor Company

Edward Lumsdaine
Michigan Technological University

Apoorv Talekar
Wayne State University

Bashar AbdulNour
Ford Motor Company

CITATION: Cash, R., Lumsdaine, E., Talekar, A., and AbdulNour, B., "An Experimental and Computational Investigation of Water Condensation inside the Tubes of an Automotive Compact Charge Air Cooler," SAE Technical Paper 2016-01-0224, 2016, doi:10.4271/2016-01-0224.

Abstract

To address the need of increasing fuel economy requirements, automotive Original Equipment Manufacturers (OEMs) are increasing the number of turbocharged engines in their powertrain line-ups. The turbine-driven technology uses a forced induction device, which increases engine performance by increasing the density of the air charge being drawn into the cylinder. Denser air allows more fuel to be introduced into the combustion chamber, thus increasing engine performance. During the inlet air compression process, the air is heated to temperatures that can result in pre-ignition resulting and reduced engine functionality. The introduction of the charge air cooler (CAC) is therefore, necessary to extract heat created during the compression process. The present research describes the physics and develops the optimized simulation method that defines the process and gives insight into the development of CACs. The present research develops a 3-D computational model using ANSYS® Fluent of the CAC internal flow with condensate and validates the predictions of the 3-D model using measurements from experimental data. Finally, the research presents a correlation that provides an approach for designing heat exchangers for practical applications that encounter moisture in the intake air stream. The overall benefit presented is an experimentally validated simulation methodology to evaluate and design CACs that function outside the condensate formation zone during vehicle operation modes.

Introduction

A charge air cooler (CAC) heat exchanger is used in conjunction with eco-boost internal combustion (IC) gasoline turbo direct injection (GTDI) and diesel engines to increase combustion output as illustrated in Figure 1.

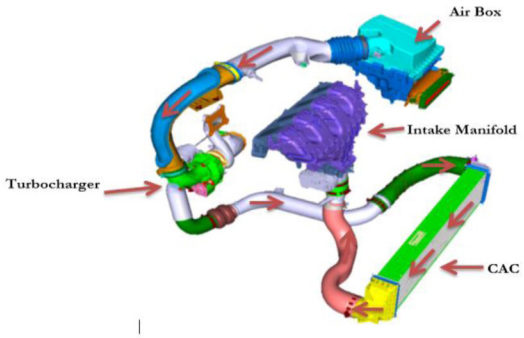

Figure 1. Air flow direction from air induction to engine intake manifold

Under the condition in which too much condensate is generated and accumulation ensues, there is a risk of the condensate being pushed into the combustion chamber during demanding engine loads, or maximum velocity with vehicle grade referred to as a wide-open throttle (WOT) condition. The ingestion of a critical mass of water into the combustion chambers can lead to misfire and other adverse effects. Currently, there is no way to accurately predict the amount of condensate formation during engine operation or the conditions under which it is formed.

According to Tang [1], a criteria is defined for condensation based on the typical CAC operation as pressure drop of 10,000 Pascal at a temperature of 20°C. Saturation temperatures increase as pressure ratios increase. Tang asserted that when reported operational conditions are met as shown in Figure 2, condensation will occur above the outlined temperature curves. The encircled red zone represents the condition currently under investigation. Experimental measurements have shown that condensation occurs in this zone; therefore additional study is needed. Tang's study does not include computational fluid dynamics (CFD) simulation or experimental correlation of the condensation mechanism.

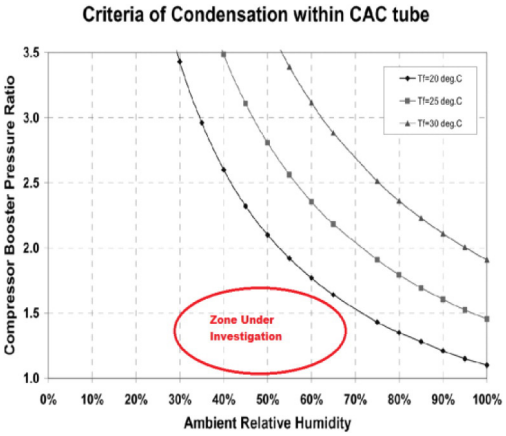

Figure 2. Reprinted with permission from SAE International. The criteria for an example charge air system, including turbo-charged CAC at 20 degrees ambient

Dalkilic and Wongwises [2] summarizes condensation studies in a comprehensive literature review inside horizontal tubes. They reported that two-pahse pressure drop is an important design parameter for heat exchangers and should also be correlated with experimental data for small channels. This asserts that two-phase pressure drop in small tubes occurs mainly due to friction, acceleration and gravitational effects of the flow. Dalkilic et al. [3] investigated heat transfer enhancement techniques for internal tube flow used by refrigeration, automotive and process industries. It was concluded that heat transfer coefficients increase with the mass flux average vapor quality of the refrigerant. Murase et al. [4] described the reduction in heat transfer performance of a given row of a bank of horizontal tubes due to the inundation of condensate falling from higher tubes to lower tubes in the bank which affected the heat transfer coefficient and thus the heat flux. Correlations were drawn between the surface quality of the tube and the effect of inundation on the heat transfer. The relationship between condensation inside the tube and the rate of the heat transfer was also established. Vyskocil et al. [5] modeled two vessels filled with several species connected by a tube. They developed a condensation model for cases where non-condensable gases are present to predict the rate of the condensation and the reduction in heat flux.

Garcia [6] studied the corrosive nature of EGR condensate in CACs that develops due to lower operating pressures due to introduction EGR in diesel engines. The acidic natural of the condensation on exhaust gases can lead to corrosion of the CAC and other components, thereby, introducing additional contaminents into the system. This work can be useful in predicting heat flux and to estimate the useful life of components and systems.

Experimental Setup

The testing rig was designed to simulate the conditions that the CAC experiences during vehicle operations in order to understand how condensate forms inside the tubes. Air flow, representing charge air, of a controlled relative humidity (RH), temperature, pressure, and air velocity rate is passed through a single tube of a CAC. The test setup in illustrated in the block diagram in Figure 3.

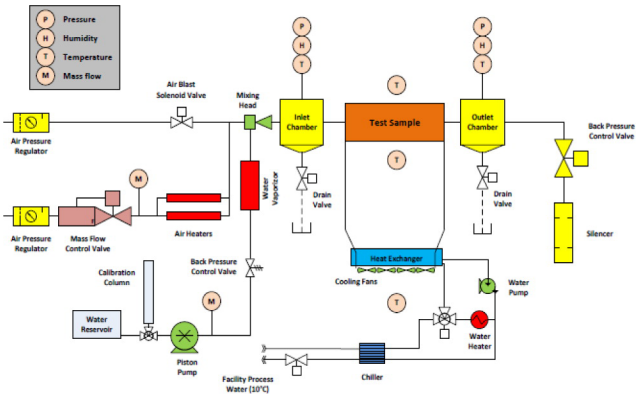

Figure 3. Block Diagram of Experimental Hardware

Table 1. Limiting Operating Parameters for the Experiment

Parameter	Maximum Operational Limit
Inlet Charge Air Temperature (°C)	80
Pressure (kPa)	353
Inlet Relative Humidity (%)	100
Charge Air Mass Flow Rate (m3/s)	.85
Outlet charge Air Temperature (°C)	80

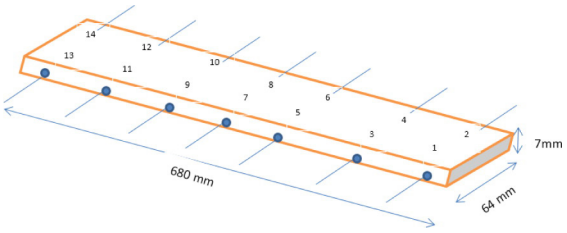

Figure 4. Positioning of the Thermocouples along the Length of the Tube

Test Protocol

The ambient conditions (temperature, pressure and RH) are recorded. The test rig is powered on and the inlet conditions (charge air inlet temperature, pressure, air velocity and RH) are set. Each test is preceded by a standard baseline. The baseline data is used to determine the consistency of the test data. The cooling rig is run for a period of 60 minutes to achieve steady-state at the baseline condition at a set RH, pressure, temperature and air velocity. Once the steady-state condition is achieved, the temperature profile is recorded for 60 minutes. Once the baseline is complete, the appropriate parameter is adjusted and run until it is stabilized (60 minutes). The amount of condensate collected in the outlet chamber of the tube was drained after every one hour of steady state test run and was volumetrically measured. The error in this measurement can be due to the thin layer of condensate remaining inside of the chamber and the CAC tube.

Simulation Setup

Kakimpa et al. [7] who used of the thin-film modeling approach to accurately predict and reproduce film thickness with lower computational cost by modeling the flow as an incompressible, Newtonian fluid for which the velocity profiles, film pressure and temperatures needed to be solved in order to determine the film flow. The Eulerian thin-film model was paired with the finite volume solution to simulate thin-film over a rotating plate. Baydu et al. [8] engage both the Eulerian multiphase and RNG k-ε models to investigate flows between a stationary shroud and rotating spiral bevel gear.

The Porous and k-epsilon RNG model to resolve velocity and pressure gradient and dissipation of kinetic energy respectfully. The near wall model (wall film)[9] is used to solve the velocity at the wall. Density based solver in ANSYS Fluent does not allow the use of velocity boundary condition hence pressure based solver was used with turbulent velocity inlet. Currently, the wall film model can resolve condensation with a User Defined Function (UDF) to account for diffusion. As such, an original UDF was written to resolve condensation. The conjugate heat transfer model [10] is used to solve for the total heat transfer and the phase change model was used to calculate the mass of the condensate and the thickness of the water film present.

The mass of water film and its thickness are two key factors in the design of systems that use compressed air. The aluminum tube with the dimensions 64 mm wide by 657 mm long by 7.8 mm tall of 0.4 mm thickness was included for this conjugate heat transfer problem. A total of 2,040,642 elements was used to discretize the entire domain including the aluminum tube, charge air (inside the aluminum tube) and external air.

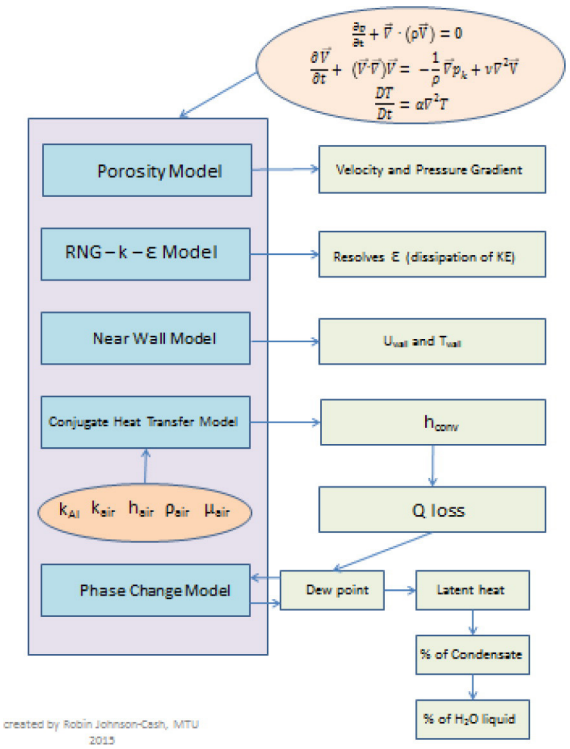

Figure 5. Schematics of the CFD Modeling

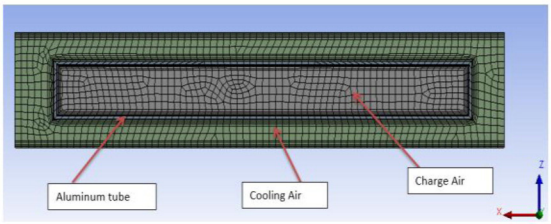

Figure 6. Mesh Cross-sectional View

Table 2. Mesh Parameters

CAC Mesh Properties			
Minimum Face Size	9.66 x 10^{-3} mm	Inflation Growth Rate	1.2
Maximum Face Size	1. 0 mm	Maximum Aspect Ratio	10.652
Transition Ratio	0.272	Number of Nodes	2,106,258
Maximum Inflation Layers	5	Number of Elements	2,040,642
y^+	1-3	Inflation Layers	5

$y^+ = y/l^*$ is a measure of boundary layer thickness, where $l_w = \nu/u_*$ and $u_* = \sqrt{\tau_w/\rho}$.

According to Pope [11], the boundary layer is divided into three sub-layers and the associated y^+ values are as given below

Viscous sub-layer $0 < {}^+ < 5$

Buffer sub-layer $5 < {}^+ < 30$

Fully turbulent sub-layer $30 < y^+ < 400 \left(\frac{y}{\delta} = 0.1 - 0.2\right)$

For this study y^+-insensitive formulation was not used, as it produces pseudo-transitional results or unphysical laminar zones and is not numerically robust for complex applications. For y^+ -sensitive formulation, the results of the first simulation indicated that the initially selected coarse mesh would not fully resolve the viscous sub-layer. Therefore the finer mesh was created as pictured in Figure 6. The case with 12 m/s and 50% RH has y+ less than five therefore the viscous sub-layer has been resolved resulting in film layer formation. A fine mesh was created and the baseline case was run on the High Performance Computational (HPC) grid. The temperature profiles were consistent with the experimental data as show in Figure 6 and did generate wall film data and contour plots. Based on these results, the fine mesh was used for the remainder of the simulations study.

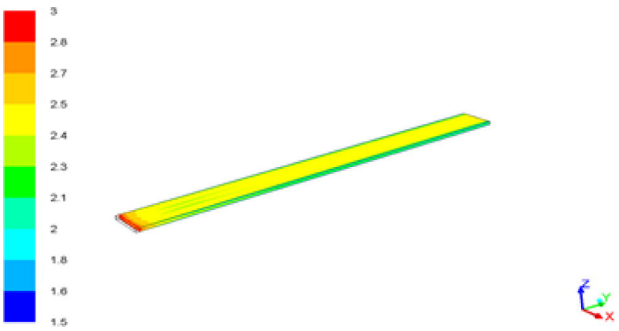

Figure 7. y^+ contours for the CAC tube refined mesh

Table 3. Boundary Conditions

Boundary Condition	Value
Inlet Charge Air Temp	55 °C
Outlet Charge Air Temp	24.7 °C
Inlet Charge Air Relative Humidity	29 %, 40 %, 50 %
Ambient Relative Humidity	50 %
Inlet Charge Air Velocity	8 m/s, 10 m/s, 12 m/s

The CAC tube has a 3.5 mm x 64 mm cross-section and has fins insides which are 1.5 mm apart. Due to the closely spaced structure of the CAC tube epsilon (dissipation term of the turbulence modelling) is difficult to resolve in the near wall region. For that k-epsilon (ε) RNG model is a good fit as it works better with the enhanced near wall treatment. RNG k-epsilon model has an R-epsilon term which is an extra term in the epsilon equation which improves the accuracy for rapidly strained flows. In rapidly strained flows, the RNG model yields a lower turbulent viscosity than the standard k-epsilon model. RNG theory provides analytical formula for the turbulent Prandtl number, where standard k-epsilon model uses constant values which makes it difficult to resolve turbulent dissipation term near the wall [11][12].

$$\frac{\partial}{\partial t}(\rho k) + \frac{\partial}{\partial x_i}(\rho k u_i) = \frac{\partial}{\partial x_j}\left(\alpha_k \mu_{eff} \frac{\partial k}{\partial x_j}\right) + G_k + G_b - \rho\varepsilon - Y_M + S_k \quad (1)$$

$$\frac{\partial}{\partial t}(\rho \varepsilon) + \frac{\partial}{\partial x_i}(\rho \varepsilon u_i) = \frac{\partial}{\partial x_j}\left(\alpha_\varepsilon \mu_{eff} \frac{\partial \varepsilon}{\partial x_j}\right) + C_{1\varepsilon}\frac{\varepsilon}{k}(G_k + C_{3\varepsilon}G_b) - C_{2\varepsilon}\rho\frac{\varepsilon^2}{k} - R_\varepsilon + S_\varepsilon \quad (2)$$

In the above equations we have

G_k = the generation of the turbulent energy due to the mean velocity gradients

G_b = the generation of turbulent kinetic energy due to buoyancy

α_k and α_ε are the inverse effective Prandtl numbers for k and ε, respectively

S_k and S_ε are user-defined parameters

$C_{1\varepsilon}$ = 1.42 and $C_{2\varepsilon}$ = 1.68

$$R_\varepsilon = \frac{C\mu\rho\eta^3\left(\frac{1-\eta}{\eta_0}\right)}{1+\beta\eta^3}\frac{\varepsilon^2}{k} \quad (3)$$

where $\eta \equiv \frac{Sk}{\varepsilon}, \eta_0 = 4.38, \beta = 0.012.$

Prandtl postulated that at high Reynolds number, close to the wall, there is a inner layer in which the mean velocity profile is determined by the viscous scales, Pope [11]. ANSYS ® Fluent makes use of the near wall law to evaluate the velocity in the region close to the wall. The enhanced near wall equation used by ANSYS ® Fluent has the following form:

The enhanced turbulent law-of-wall [13][14] for compressible flow is as follows:

$$\frac{du^+_{turb}}{dy^+} = \frac{1}{\kappa y^+}\left[S'(1 - \beta u^+ - \gamma(u^+)\right]^{1/2}$$

$$S' = 1 + \alpha y^+ \quad (4)$$

where $\alpha = \frac{\mu}{\rho^2(u^*)^3}\frac{dp}{dx}$

$\beta = \frac{\sigma_t q_w}{\rho c_p u^* T_w}$ and $\gamma = \frac{\sigma_t (u^*)^2}{2\, c_p T_w}$

κ = von Kármán constant (= 0.4187)

μ = dynamic viscosity of the fluid.

If α, β, and γ are set to zero, then equation 4 acts as a regular law-of-wall.

Experimental Results

CAC tube inlet air velocities of 8 m/s, 10 m/s and 12 m/s represnet vehicle crusing speeds between 55 mph and 70 mph in which condensate is created inside the CAC. Hence these cases were investigated for different relative humidity, Table 4. The outlet temperature of the turbocharger provides a constant temperature air at 55 °C hence it is maintained constant for all the cases. Also the inlet temperature requirement of the engine is around 25 °C hence outlet temperature of the CAC tube is maintained constant at 25 °C.

Table 4. Experimental Cases

Velocity $_{in}$ m/sec	Temp $_{in}$ °C	RH $_{in}$ %	Cooling Air Velocity $_{in}$ m/s	Temp $_{out}$ °C
10	55	30	2	25
10	55	40	2	25
10	55	50	2	25
12	55	30	2	25
12	55	40	2	25
12	55	50	2	25
8	55	30	2	25

Determining the steady-state region of the test is necessary as this data will be correlated to the simulation results. The cooling test rig is comprised of several electronically controlled mechanical components that result in a system control system response delay. There is then a transient region followed by the steady-state region. The determination of thermal time constant (τ), is resolved to identify the steady-state region of the experimental test data. Ressler et al. [15] indicates that τ provides a measure of a systems' rate of response to input. Further, τ is the time that it takes the experimental system to reach 63.2% of the steady-state value relative to its initial value. The time constant to steady-state is given by by equation:

$$T(t) = T_{ss} + (T_o - T_{ss})e^{-\frac{t}{\tau}}(x) \quad (5)$$

The baseline condition of 10 m/s, 30% RH and 55 °C inlet charge air was used in determining the time constant of the cooling rig. The time to achieve steady-state for the charge air inlet temperature is τ = 40 mins. Figure 8 illustrates the measured-to-actual temperature in non-dimensional time, t/τ.

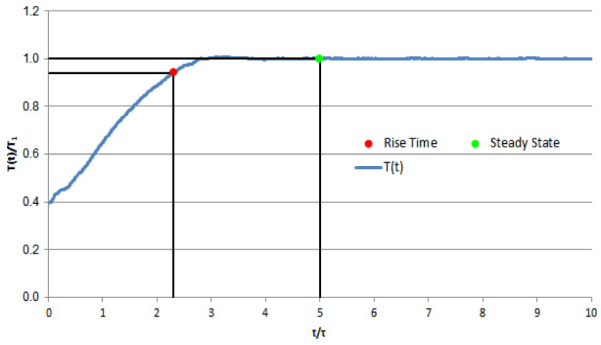

Figure 8. Measure to actual temperature in non-dimensional time t/τ

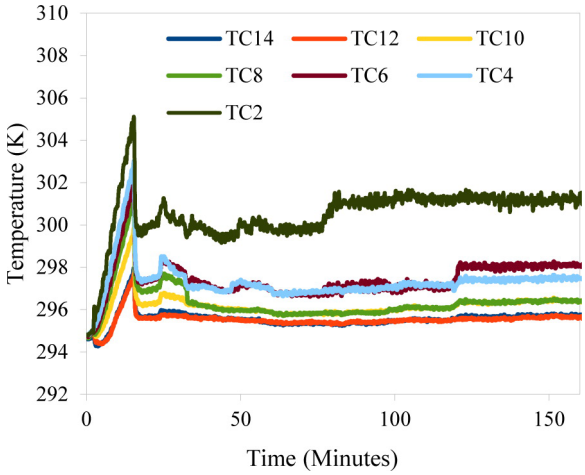

Figure 9. Even Thermocouple Data (Leading Edge of CAC Tube) for 8 m/s and 30 % RH

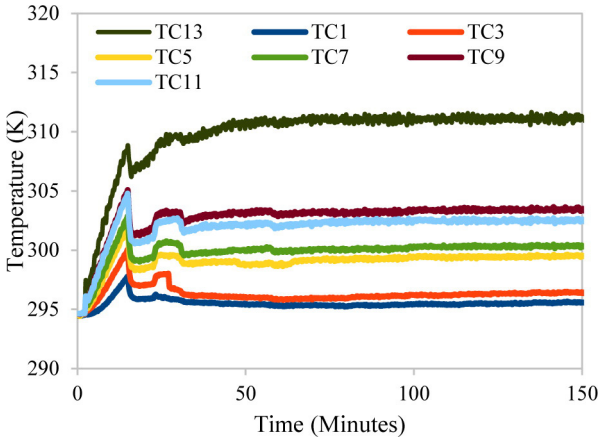

Figure 10. Odd Thermocouple Data (Rear Edge of CAC Tube) for 8 m/s and 30% RH

Figure 9 and 10 show the thermocouple transient data for 8 m/s and 30% RH case and this case yields least amount of condensate.

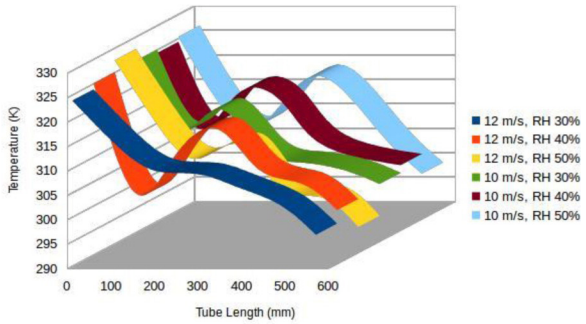

Figure 11. Temperature Vs Length of the tube for all the cases

Condensation inside the tube occurred for all the cases in practice. The minimum temperature at which condensation occurs is 305 K. Once the film forms the surface heat transfer coefficient drops suddenly as the film layer is also now offering thermal resistance. Figure 11 shows the temperature distribution along the length of the tube for first 6 cases. The minima and maxima for the curves shown in the Figure 11 defines the zone for the condensation at that particular velocity. The simulation predicted the amount of condensate formation and presented a flow pattern for all cases with charge air inlet velocity of 12 m/s as reported in Table 5.

Table 5. Condensate Values from CFD Simulation and Experiment

Velocity m/s	RH %	Condensate ml/hr.	Experimental ml/hr.
12	30	19.2	18
12	40	32.05	29
12	50	51.2	44

The minima and maxima for the curves shown in the Figure 11 define the zone for the condensation at that particular velocity, relative humidity and cooling air velocity is constant for all cases as 2 m/s. Simulation results over predict the amount of the condensation. Also there is a small amount of error in the experimental measurement of the condensate mass as tube walls has some film mass retained even after the measurement is stopped.

Analysis

The simulation accurately predicted the temperature profile for all cases. The simulation predicted the amount of condensate formation and presented a flow pattern for all cases with charge air inlet velocity of 12 m/s as reported in Table 5.

Simulations were run and the experimental mean temperature data was then compared to the steady state turbulence simulation results as shown in Figures 12 and 13. The full error analysis discussion is available in Chapter 6 of sited dissertation [16]. The error bars indicate the maximum and minimum mean temperatures recorded by the designated thermocouple and demonstrates experimental correlation to the simulation results. The thermocouples at the both end of the tube show slightly lower temperatures (1 °C) and is outside the experimental data range. The subject thermocouples are in close proximity to the air boxes as shown in the block diagram of the experimental setup in Figure 3. These boxes create a cooling effect but are helpful to reduce the swirling effects of the pumped air and regulate the air flow into the CAC tube. The inlet and outlet air chambers/boxes were not part of 3-D CFD model therefore the initial

swirling effect of air in the inlet chamber was neglected for simplicity. The inlet boundary conditions for the CAC tube (temperature, RH, and velocity) were used for initial conditions.

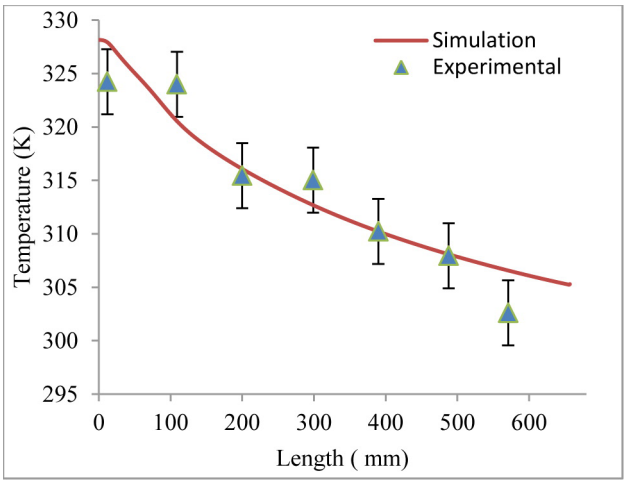

Figure 12. Correlation of experimental to coarse simulation for 10 m/s and RH 30%

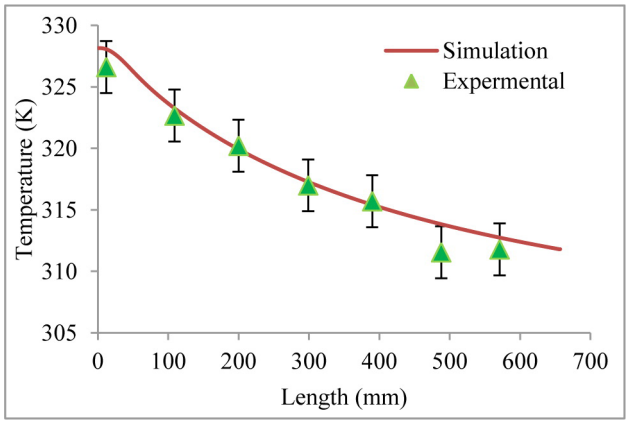

Figure 13. Correlation of experimental to fine simulation for 10 m/s and RH 40%

Figure 14 shows the condensation in terms of the inner wall film thickness for the 12 m/s and 40% relative humidity case. After reaching steady-state turbulence, the film of maximum thickness, which is 24 µm, develops at the rear face of the tube near the outlet. This shows that condensate is forming and being reconstituted or push and puddling at the exit end of the tube. This is due to the wall film motion with the air flow and the surface heat transfer coefficient which changes along the length of the tube. Figure 15 shows almost twice (41.3 µm) the film thickness due to a 10% increase in relative humidity. The area covered by the wall film is 1.5 times more compared to the previous case.

Experimental data was collected for total mass creation after one hour for the 50% RH, 12 m/s condition. By integrating the film mass over the surface area of the tube and time, the total condensation mass was calculated. The values were compared to the amount collected during the laboratory experiment for the same charge air inlet velocity, cooling air mass flow rate and relative humidity of both air streams. The results are listed in Table 5.

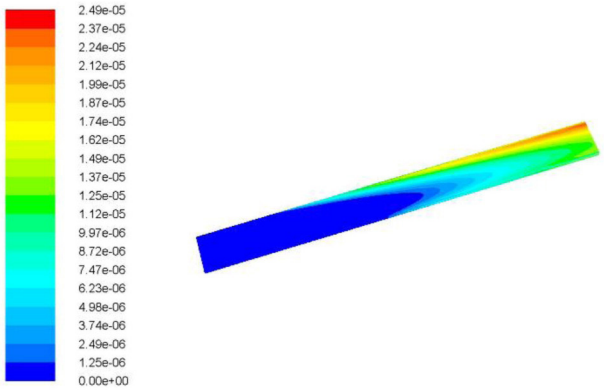

Figure 14. Film Thickness of the Wall Film (m) for 12 m/s and RH 40%

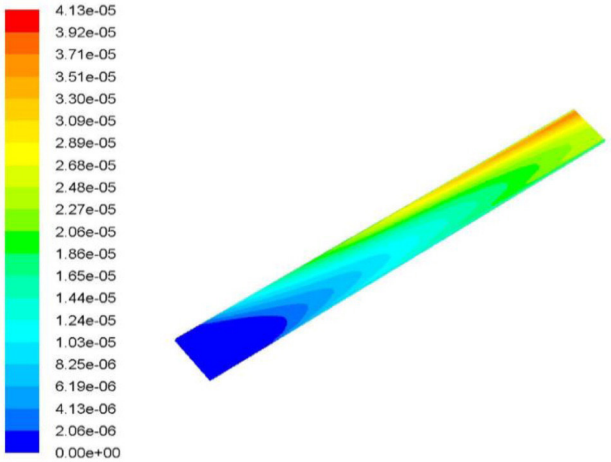

Figure 15. Film thickness of the wall film (m) for 12 m/s and RH 50%

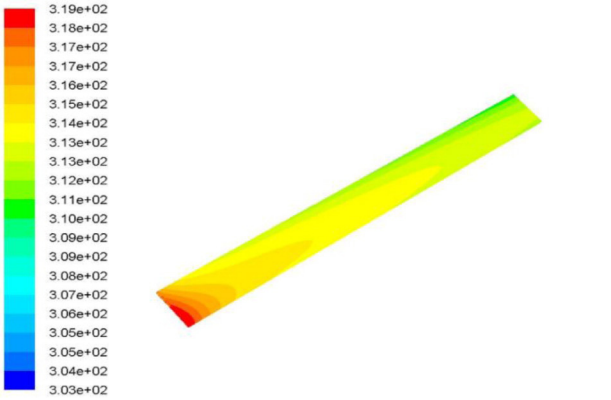

Figure 16. Temperature of the inner-wall for 12 m/s and RH 50%

The surface heat transfer coefficient and heat flux on the inner wall was compared for 12 m/s at 40% RH to 50% RH. Higher RH leads to more condensate and greater film thickness. The additional condensate created a larger heat transfer coefficient and more heat transfer resulting in higher film temperatures as shown in Figures 17, 18, 19.

In Figure 17, at x = 0 m when the cooling air initially comes in contact with the tube and there is heat flux going out of the tube and this heat flux reduces as the cooling air progresses further across the width of the tube (x = 0.064 m). The heat lost by the charge air to the cooling air is considered as negative heat flux. The direction on heat flux is reversed (positive heat flux) at the midsection of the tube (x = 0.032 m) which means the cooling air gives some of the collected heat back to the tube while passing over the tube. The effect of the relative

humidity is still significant in total heat flux. Boosted engines increase the system pressure which leads to increased dew-point temperatures. The front side of the CAC tube is exposed to the cooling air first and hence has more heat transfer than any other surface. The Eulerian film assumes the temperature of the metal boundary and heat transfer coefficient changes with the temperature of the film.

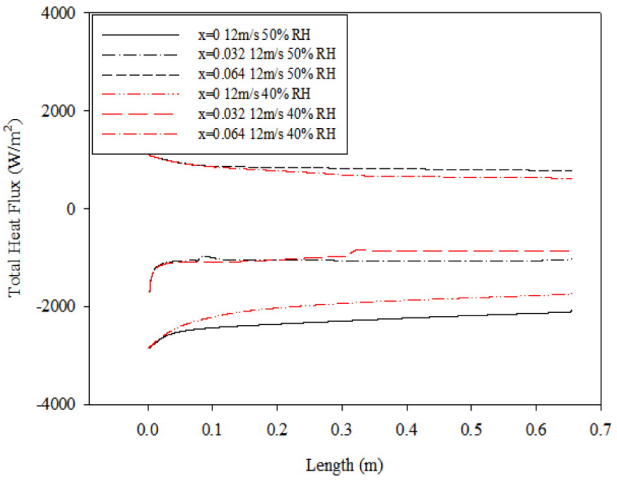

Figure 17. Total Surface Heat Flux 12 m/s and 50% RH vs 12 m/s 40% RH

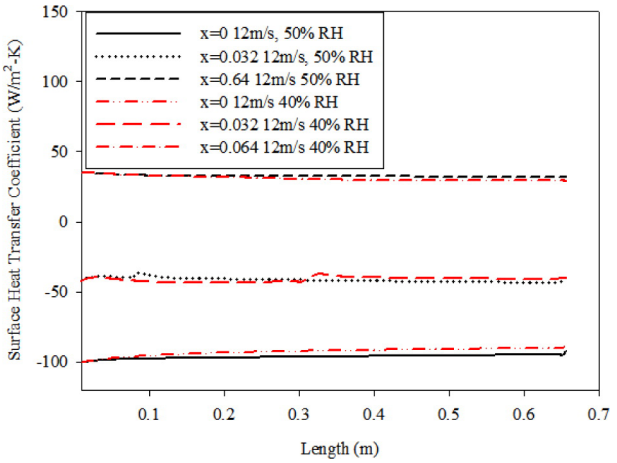

Figure 18. Surface Heat Transfer Coefficient 12 m/s and 50% RH vs 12 m/s 40% RH

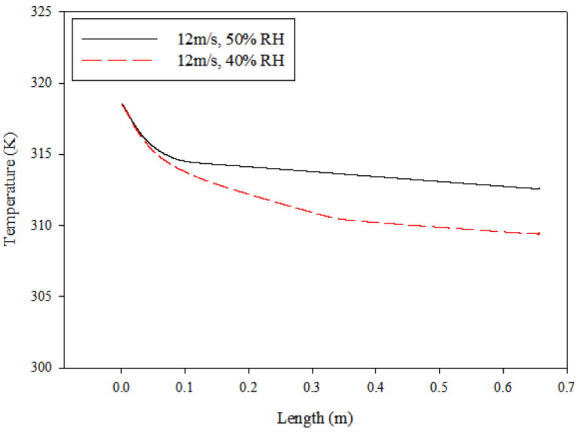

Figure 19. Wall Temperature 12 m/s and 50% RH vs 12 m/s 40% RH

The outlined experimentally validated simulation methodology illustrated in Figure 21 can be used to evaluate and design CACs that function outside the condensate formation zone during operation modes. A methodology for the design of CAC that provide maximum thermal performance without generation of a critical mass of condensate.

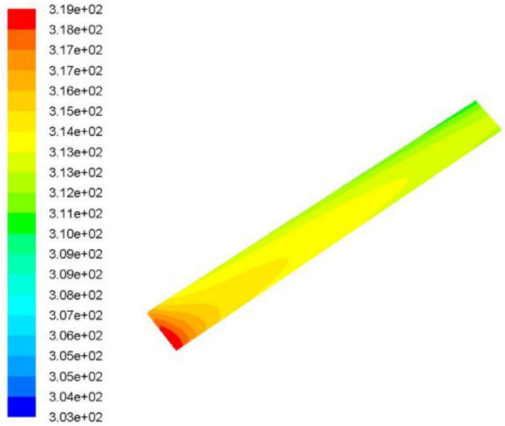

Figure 20. Wall film temperature (K) for 12 m/s and RH 50%

Wall film acquires the temperature of the wall when it forms and which is evident from Figure 16, 19 and 20. Wall temperature also changes with the motion of the wall film.

The Methodology is based on the following:

1. Development of a 3-D computational model of the CAC internal flow with condensate using ANSYS ® Fluent.
2. The simulation was validated by measurements from a Ford Motor Company experimental data which showed correlation.

Providing a validated simulation methodology for designing heat exchangers for practical applications that encounter moisture in the powertrain air intake air stream.

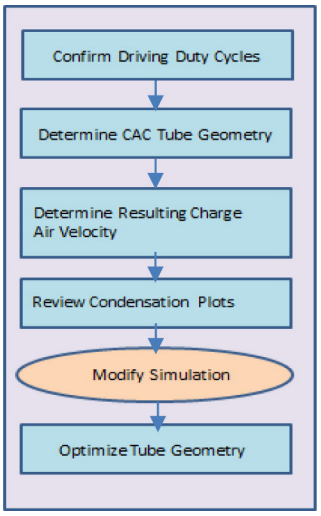

Figure 21. Steps of the Validated Simulation Methodology

Conclusions

1. As the velocity of the inlet charged air is increased the condensate quantity increases for the same area of the CAC tube wall.
2. Increase in relative humidity is a major factor in the condensation formation along with the velocity of the air.

3. Condensate formation is predominant once the steady state is reached and is evident also from the transient simulation that after 100 seconds of the steady turbulence in real time condensate mass reaches the steady formation rate.
4. Wall film formation and evaporation are the concurrent processes and relative humidity, surface heat transfer coefficient and finned surface area are some of the very important factors which decide the speed of these two processes. More investigation is needed to calculate the relation between evaporation rate and the condensate formation speed inside the CAC tube for varying cooling air temperature.
5. RNG k-ε turbulence modelling with Eulerian film model gives satisfactory results in terms of the film mass, thickness and the movement of the wall film. But to obtain realistic values for the film thickness enhanced wall treatment is most suitable but computationally expensive method. A new computational model is tested and established for predicting condensation amount and location in finned structure of CAC tube.
6. y^+ in this simulation is in the range 1-3 and which results in the resolved viscous sub-layer near wall region which is the predominant region for the wall film accumulation. Stripping and movement of the wall film is highly mesh sensitive. In this case mesh independence has been achieved for given boundary conditions.

References

1. Tang, Y., "The Condensation within a CAC - Thermodynamics Analysis," SAE Technical Paper 2011-01-1168, 2011, doi:10.4271/2011-01-1168.
2. Dalkilic, A.S. and Wongwises, S., "Intensive literature review of condensation inside smooth and enhanced tubes," *Int. J. Heat Mass Transf.* 52(15-16):3409-3426, 2009, doi:10.1016/j.ijheatmasstransfer.2009.01.011.
3. Dalkilic, A.S., Celen, A., Awad, M.M., and Wongwises, S., A Critical review on the determination of convective heat transfer coefficient during condensation in smooth and enhanced tubes, Heat Transf. Summer Conf., 2013.
4. Murase, T., Wang, H.S., and Rose, J.W., "Effect of inundation for condensation of steam on smooth and enhanced condenser tubes," *Int. J. Heat Mass Transf.* 49(17-18):3180-3189, 2006, doi:10.1016/j.ijheatmasstransfer.2006.02.003.
5. Vyskocil, L., Schmid, J., and Macek, J., "CFD simulation of air-steam flow with condensation," *Nucl. Eng. Des.* 279:147-157, 2014, doi:10.1016/j.nucengdes.2014.02.014.
6. Garcia, J., "Exhaust Gas Condensate Corrosion Test on Low Pressure Cooling System of Aluminum Brazed EGR, ACAC and WCAC," SAE Technical Paper 2012-01-1947, 2012, doi:10.4271/2012-01-1947.
7. Kakimpa, B., Morvan, H.P., and Hibberd, S., "Thin-Film Flow Over a Rotating Plate: An Assessment of the Suitability of VOF and Eulerian Thin-Film Methods for the Numerical Simulation of Isothermal Thin-Film Flows," ASME Turbo Expo 2015: Turbine Technical Conference and Exposition, V05CT15A027-V05CT15A027, 2015.
8. Al Baydu C., K.S. and H.P.M., "Two-Phase Computational Modelling of a Spiral Bevel Gear Using a Eulerian Multiphase Model," ASME Turbo Expo 2015: Turbine Technical Conference and Exposition, 10, 2015.
9. AbdulNour, B., "Numerical Simulation of Vehicle Defroster Flow Field," SAE Technical Paper 980285, 1998, doi:10.4271/980285.
10. Patankar, S. V., "Numerical Heat Transfer and Fluid Flow," Hemisphere, Washington, DC., 1980.
11. Pope, S.B., "Turbulent Flows," Cambridge University press, ISBN 978-0521598866, 2000.
12. Orszag, S. A., Yakhot, V., Flannery, W. S., Boysan, F., Choudhury, D., Maruzewski, J., & Patel, B., "Renormalization Group Modeling and Turbulence Simulations," *Near-wall turbulent flows*, 1031-1046, 1993.
13. White, F. and Christoph, G., "A Simple New Analysis of Compressible Turbulent Two-Dimensional Skin Friction Under Arbitrary Conditions," 1971.
14. Huang P., Bradshaw P., and T.C., "Skin friction and velocity profile family for compressible turbulentboundary layers," *AIAA J.* 31(9):1600-1604, 1993.
15. Ressler, K., Brucker, K., and Nagurka, M., "A Thermal Time-Constant Experiment *," *Int. J. Eng. Educ.* 19(4), 2003.
16. Cash, Robin, "A Quantitative Investigation of the Water Condensation Inside Tubes of Compact Charge Air Cooler", Open Access Dissertation, Michigan Technological University, 2015.

Contact Information

Robin Y Johnson-Cash
Ford Motor Company
15011 Commerce Drive
Dearborn, MI 48120
rcash@ford.com

Acknowledgements

The authors would like to thank Dr. Jeffery S. Allen (Michigan Technological University) and Dr. Song-Lin Yang (Michigan Technological University) for their valuable and precise suggestions related to the experimental and simulation procedures, respectively, and for the Ford Motor Company for making available the research facilities and the high performance computing grid, as well as the practical test data.

The Engineering Meetings Board has approved this paper for publication. It has successfully completed SAE's peer review process under the supervision of the session organizer. The process requires a minimum of three (3) reviews by industry experts.

ISSN 0148-7191

http://papers.sae.org/2016-01-0224